Supporting Information

Seven-coordinate Ln^{III} Complexes Assembled from a Bulky ^{Mes}acacH Ligand: Synthesis, Structure, Photoluminescence and SMM behaviour

Pankaj Kalita,[a,b] Prakash Nayak,[a] Naushad Ahmed,[b] Juan Manuel Herrera,[c] Krishnan Venkatasubbaiah,[a] Enrique Colacio,[c]* and Vadapalli Chandrasekhar*[b,d]*

[a]School of Chemical Sciences, National Institute of Science Education and Research Bhubaneswar, HBNI, Jatni, Khurda - 752050, Odisha, India

[b]Tata Institute of Fundamental Research Hyderabad, Gopanpally, Hyderabad-500 046, India

[c]Departamento de Química Inorgánica, Facultad de Ciencias, Universidad de Granada, Avenida de Fuentenueva s/n, 18071 Granada, Spain

[d]Department of Chemistry, Indian Institute of Technology Kanpur, Kanpur-208016, India

AUTHOR EMAIL ADDRESSES: vc@iitk.ac.in; vc@tifrh.res.in; krishv@niser.ac.in
ecolacio@ugr.es

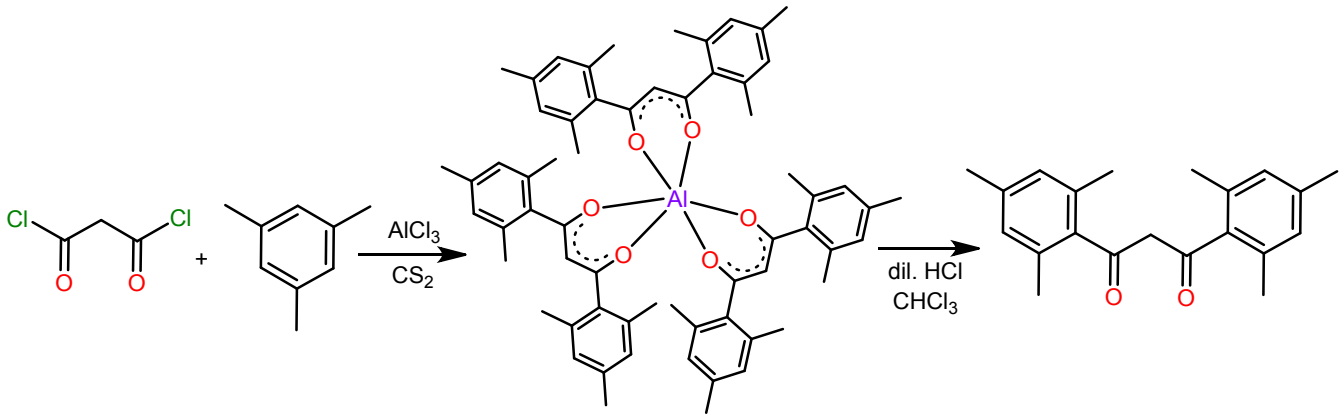

Scheme S1. Synthetic reaction scheme for the preparation of ^{Mes}Acac ligand.

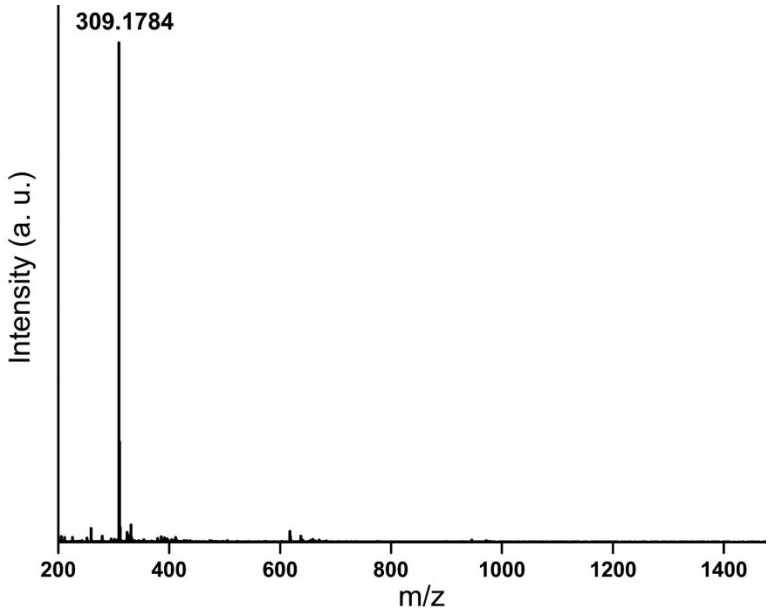

Fig. S1. ESI-MS of ^{Mes}Acac ligand

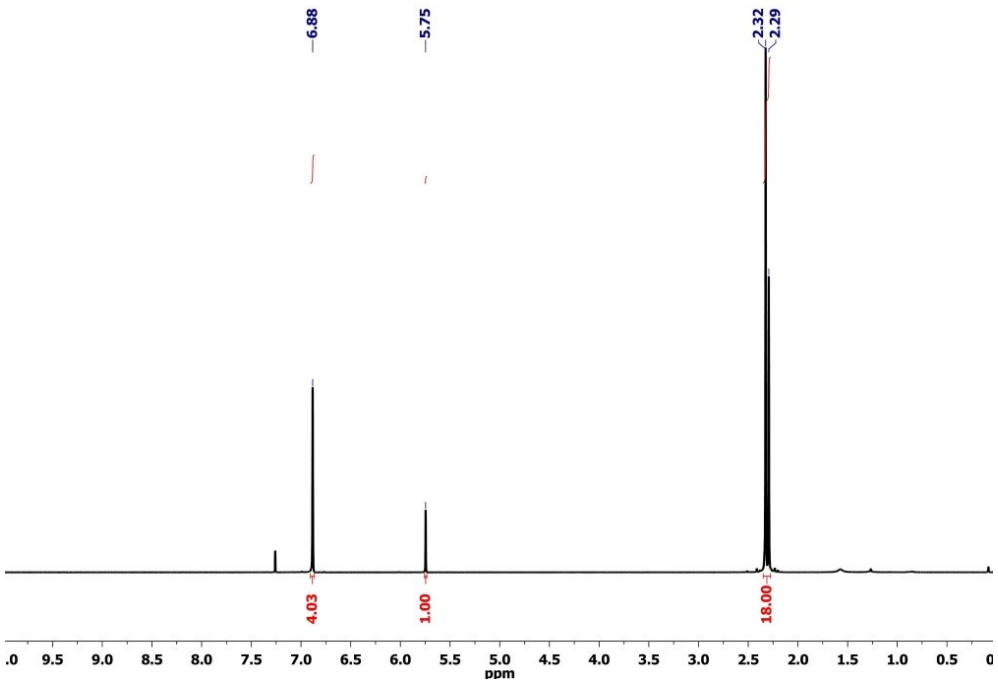

Fig. S2. ^{1}H nmr spectra of ^{Mes}Acac. (The signal at 7.26 is due to the residual solvent)

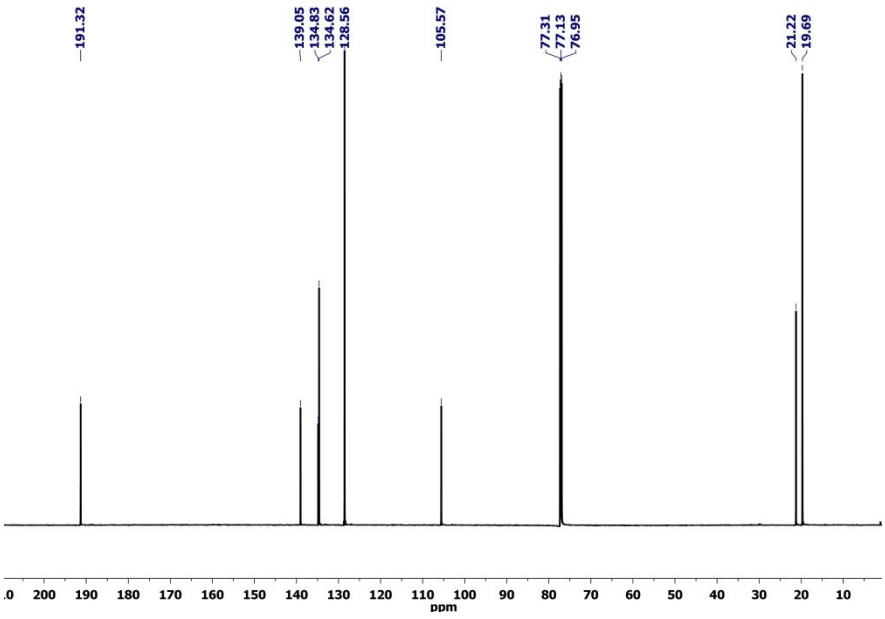

Fig. S3. ^{13}C{^{1}H}nmr spectra of ^{Mes}Acac. (The signals at 76-77 are due to the residual solvent)

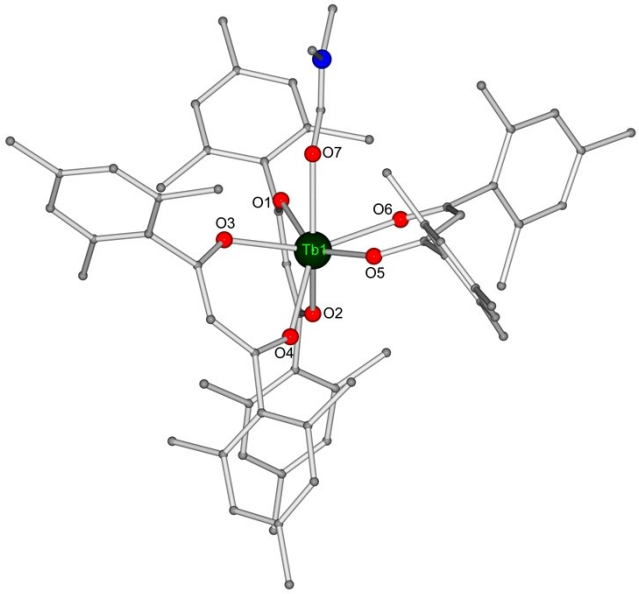

Fig. S4. (*top*) Molecular structure of complex **2**; (*bottom*) piano stool coordination geometry around the Tb^{III} centre. Colour codes: C = grey; N = blue; O = red; Tb = olive green (H atoms are omitted for clarity).

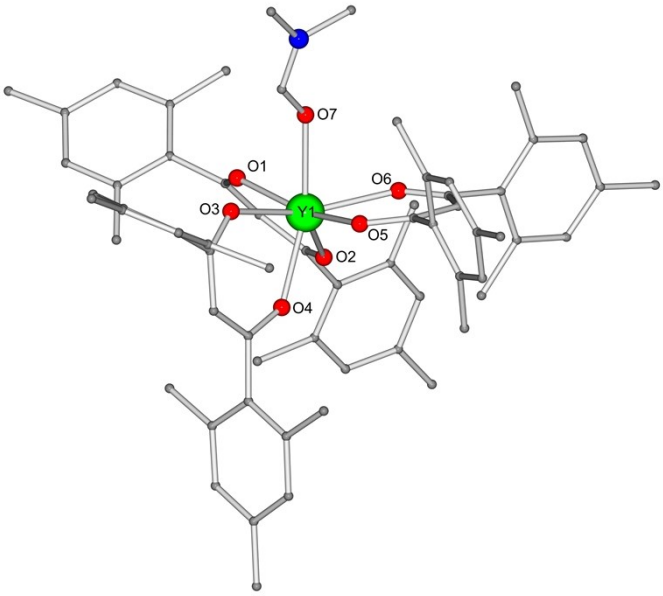

Fig. S5. (*top*) Molecular structure of complex **3**; (*bottom*) piano stool coordination geometry around the $(Y_{0.91}/Dy_{0.09})^{III}$ centre. Colour codes: C = grey; N = blue; O = red; $Y_{0.09}Dy_{0.91}$ = bright green (H atoms are omitted for clarity).

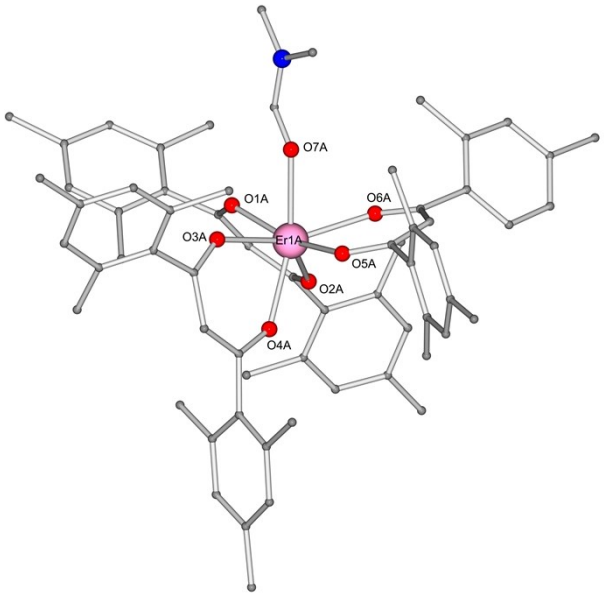

Fig. S6. (*top*) Molecular structure of complex **4**; (*bottom*) piano stool coordination geometry around the Er^{III} centre. Colour codes: C = grey; N = blue; O = red; Er = plum (H atoms are omitted for clarity)

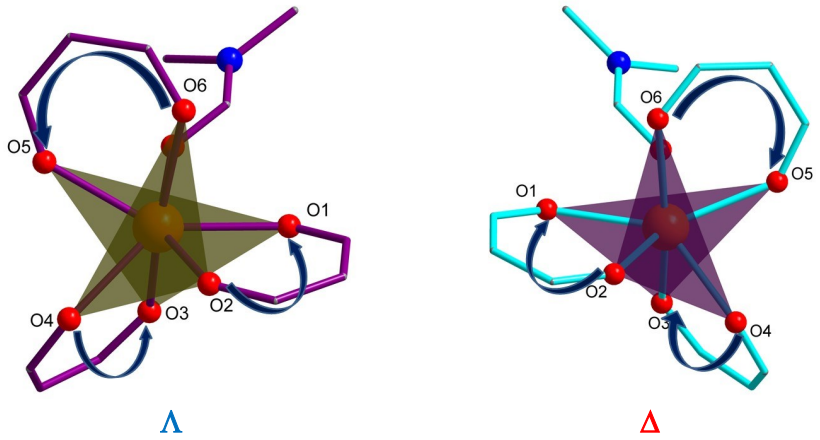

Fig. S7. Λ and Δ isomers of complex **1** (only the core view is shown for clarity and the coordinating DMF molecule is ignored in assigning the helicity of the isomers).

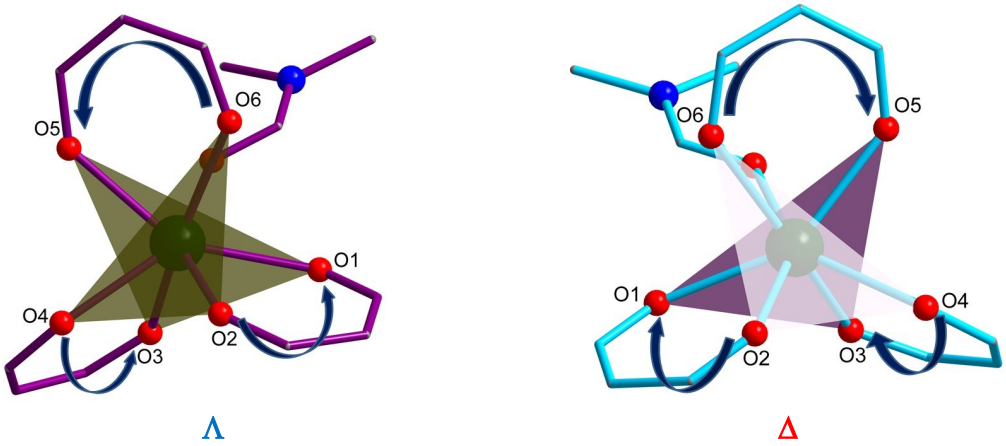

Fig. S8. Λ and Δ isomers of complex **2** (only the core view is shown for clarity and the coordinating DMF molecule is ignored in assigning the helicity of the isomers).

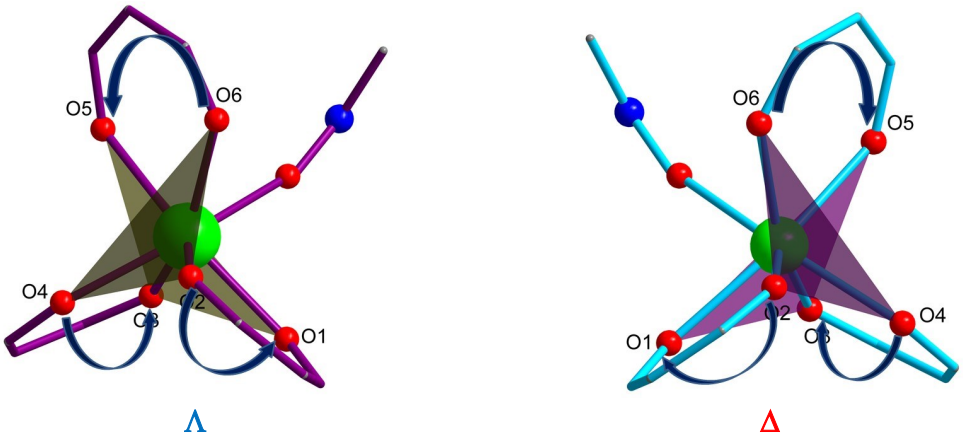

Fig. S9. Λ and Δ isomers of complex **3** (only the core view is shown for clarity and the coordinating DMF molecule is ignored in assigning the helicity of the isomers).

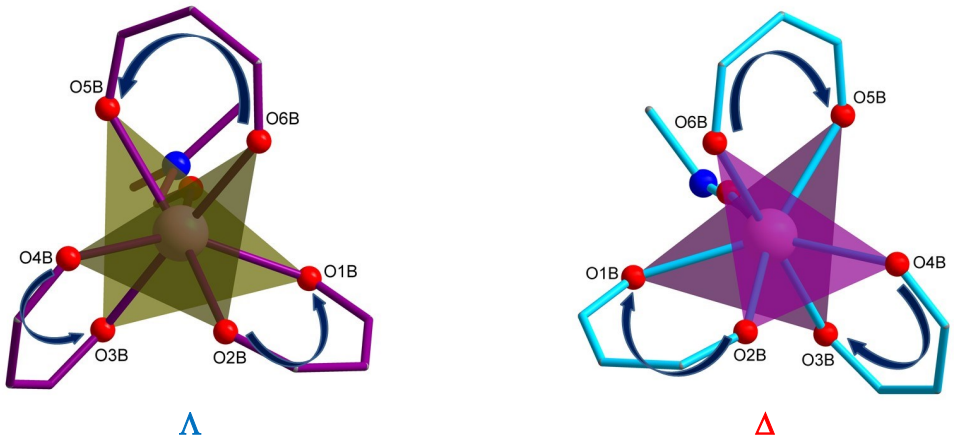

Fig. S10. Λ and Δ isomers of complex **4** (only the core view is shown for clarity and the coordinating DMF molecule is ignored in assigning the helicity of the isomers).

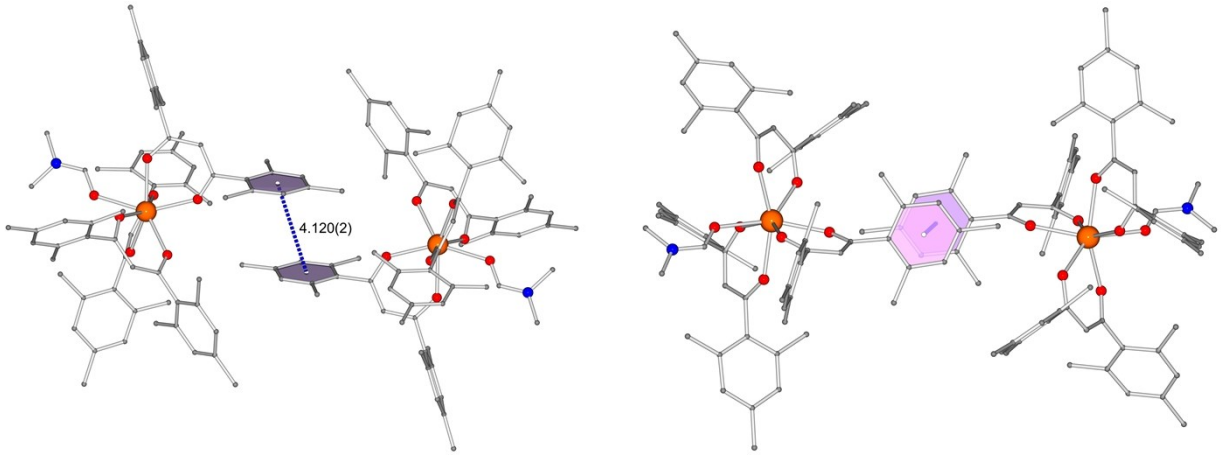

Fig. S11. Sandwich-type pi-pi stacking of mes rings, with the inversion center of the *P*–1 unit cell being sited along the ring centroid vector of **1**. The centroid·····centroid distance between the two rings is 4.120(3) Å. (H atoms are omitted for clarity)

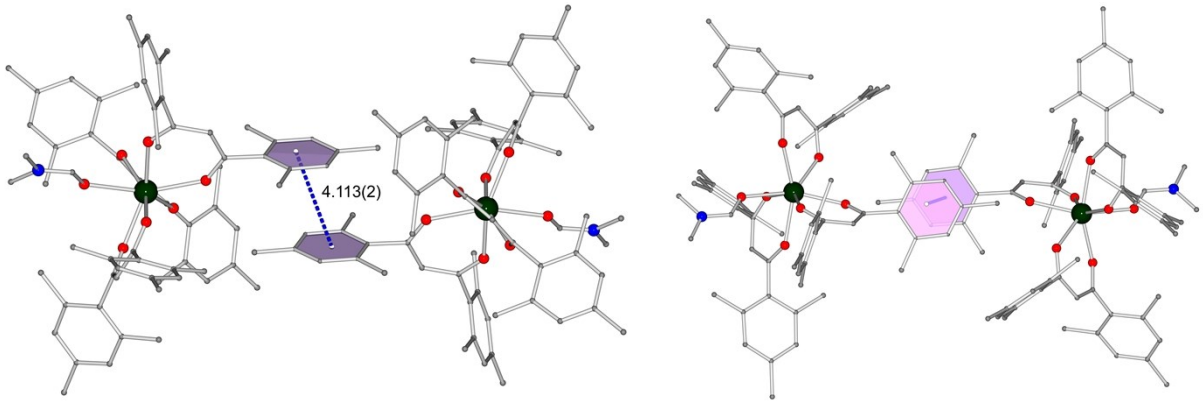

(*side view*) (*top view*)

Fig. S12. Sandwich-type pi-pi stacking of mes rings, with the inversion center of the *P*–1 unit cell being sited along the ring centroid vector of **1**. The centroid·····centroid distance between the two rings is 4.113(2) Å. (H atoms are omitted for clarity)

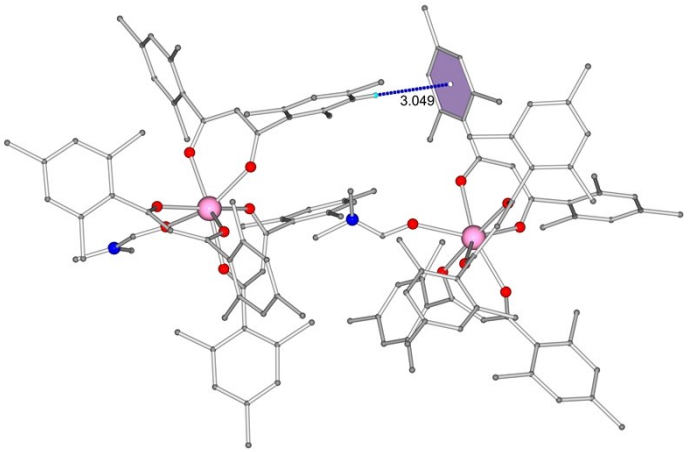

Fig. S13. Sandwich-type pi-pi stacking of mes rings, with the inversion center of the *P*–1 unit cell being sited along the ring centroid vector of **1**. The centroid·····centroid distance between the two rings is 4.113(2) Å. (H atoms are omitted for clarity)

Table S1. The Continuous Shape Measures calculations using SHAPE program for different probable coordination geometries with C.N. 7 around the Ln(III) centre of **1**–**4**.

Complex	Structure†						
	HP-7	HPY-7	PBPY-7	**COC-7**	**CTPR-7**	JPBPY-7	JETPY-7
1_Dy CShM	33.207	21.365	6.096	**0.675**	1.506	9.512	16.499
2_Tb CShM	33.050	21.423	6.185	**0.712**	1.533	9.626	16.300
3_Dy CShM	33.906	21.193	6.279	**0.620**	1.162	9.969	16.768
4_Er1A CShM	35.253	19.894	5.631	**0.646**	1.604	9.321	19.036
Er1B CShM	36.145	20.421	3.087	2.654	**2.280**	6.712	20.434

† HP-7 = Heptagon (D7h); HPY-7 = Hexagonal pyramid (C6v); PBPY-7 = Pentagonal bipyramid (D5h); COC-7 = Capped octahedron (C3v); CTPR-7 = Capped trigonal prism (C2v); JPBPY-7 = Johnson pentagonal bipyramid J13 (D5h); JETPY-7 = Johnson elongated triangular pyramid J7 (C3v)

Table S2. Selected bond lengths (Å) and bond angle (°) for the complex **2**, **3**, and **4**

Complex with C.G.	**Bond lengths** (Å)	**Bond angles** (°)
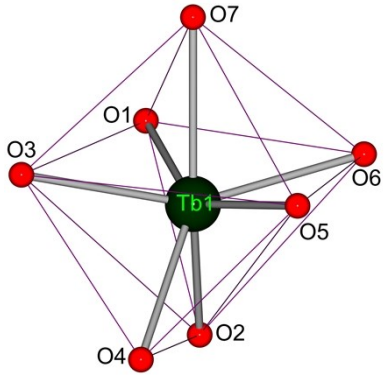 Distorted capped octahedron geometry of *Tb1* in complex **2**	Tb1−O1 2.3082(12) Tb1−O2 2.2878(14) Tb1−O3 2.2929(14) Tb1−O4 2.3166(13) Tb1−O5 2.2852(13) Tb1−O6 2.3200(15) Tb1−O7 2.3959(14)	O1−Tb1−O4 134.99(5) O1−Tb1−O6 82.11(5) O1−Tb1−O7 76.94(5) O2−Tb1−O1 74.22(5) O2−Tb1−O3 112.02(6) O2−Tb1−O4 75.13(5) O2−Tb1−O6 87.20(6) O2−Tb1−O7 149.52(5) O3−Tb1−O1 88.37(5) O3−Tb1−O4 73.62(5) O3−Tb1−O6 155.39(6) O3−Tb1−O7 76.53(6) O4−Tb1−O6 128.18(5) O4−Tb1−O7 134.19(5) O5−Tb1−O1 148.64(5) O5−Tb1−O2 123.20(5) O5−Tb1−O3 105.35(5) O5−Tb1−O4 76.36(5) O5−Tb1−O6 73.78(5) O5−Tb1−O7 79.06(5) O6−Tb1−O7 79.22(6)
		O1−Y1−O2 73.96(7) O1−Y1−O3 86.34(8)

<table>
<tr>
<td> 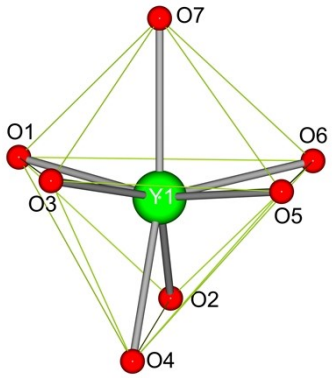

Distorted capped octahedron geometry of Y1 in complex 3</td>
<td>Y1–O1 2.262(2)
Y1–O2 2.306(2)
Y1–O3 2.329(2)
Y1–O4 2.255(2)
Y1–O5 2.336(2)
Y1–O6 2.270(2)
Y1–O7 2.336(2)</td>
<td>O1–Y1–O5 160.02(7)
O1–Y1–O6 113.79(8)
O1–Y1–O7 81.63(8)
O2–Y1–O3 138.03(7)
O2–Y1–O5 125.87(7)
O2–Y1–O7 132.75(8)
O3–Y1–O5 79.27(7)
O3–Y1–O7 77.96(7)
O4–Y1–O1 105.38(8)
O4–Y1–O2 75.07(8)
O4–Y1–O3 75.09(7)
O4–Y1–O5 84.34(8)
O4–Y1–O6 118.07(8)
O4–Y1–O7 151.55(8)
O5–Y1–O7 81.87(8)
O6–Y1–O2 72.30(8)
O6–Y1–O3 149.07(8)
O6–Y1–O5 74.78(7)
O6–Y1–O7 81.95(8)</td>
</tr>
<tr>
<td> 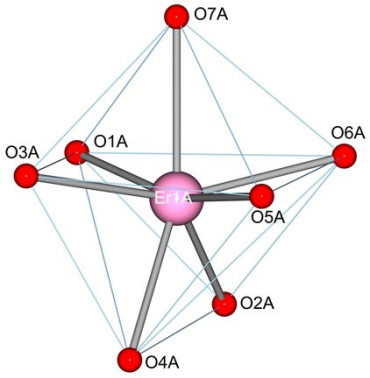

Distorted capped octahedron geometry of Er1A in complex 4</td>
<td>Er1A–O1A 2.256(2)
Er1A–O2A 2.266(2)
Er1A–O3A 2.260(2)
Er1A–O4A 2.274(2)
Er1A–O5A 2.278(2)
Er1A–O6A 2.268(2)
Er1A–O7A 2.335(2)</td>
<td>O1A–Er1A–O2A 73.63(8)
O1A–Er1A–O3A 83.03(8)
O1A–Er1A–O4A 109.60(9)
O1A–Er1A–O5A 162.63(8)
O1A–Er1A–O6A 107.65(9)
O1A–Er1A–O7A 79.26(9)
O2A–Er1A–O4A 76.59(8)
O2A–Er1A–O5A 122.79(8)
O2A–Er1A–O6A 73.89(9)
O2A–Er1A–O7A 131.75(9)
O3A–Er1A–O2A 133.47(8)
O3A–Er1A–O4A 74.24(8)
O3A–Er1A–O5A 87.80(8)
O3A–Er1A–O6A 152.56(9)
O3A–Er1A–O7A 79.95(8)
O4A–Er1A–O5A 81.80(9)
O4A–Er1A–O7A 151.18(9)
O5A–Er1A–O7A 84.64(9)
O6A–Er1A–O4A 122.54(9)
O6A–Er1A–O5A 74.79(8)
O6A–Er1A–O7A 77.49(9)</td>
</tr>
<tr>
<td></td>
<td>Er1B–O1B 2.304(2)
Er1B–O2B 2.272(2)
Er1B–O3B 2.252(2)
Er1B–O4B 2.286(2)
Er1B–O5B 2.297(2)
Er1B–O6B 2.271(2)</td>
<td>O3B–Er1B–O1B 96.34(9)
O3B–Er1B–O2B 91.21(9)
O3B–Er1B–O4B 75.17(8)
O3B–Er1B–O5B 107.78(9)
O3B–Er1B–O6B 176.67(8)
O3B–Er1B–O7B 77.8(4)
O4B–Er1B–O1B 147.25(8)
O4B–Er1B–O5B 76.37(8)
O4B–Er1B–O7B 132.8(3)
O5B–Er1B–O1B 135.53(8)
O6B–Er1B–O1B 83.88(9)</td>
</tr>
</table>

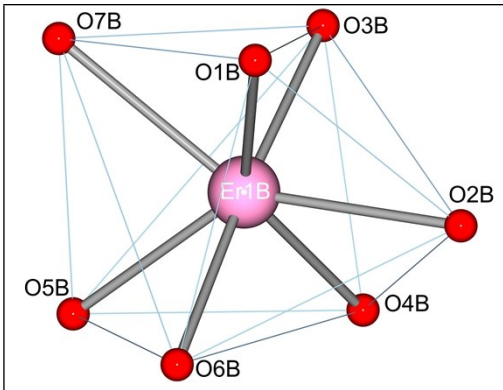 Distorted capped trigonal prism geometry of *Er1B* in complex **4**	Er1B–O7B 2.312(4)	O6B–Er1B–O2B 85.65(9) O6B–Er1B–O4B 102.87(8) O6B–Er1B–O5B 74.12(8) O6B–Er1B–O7B 105.5(4) O1B–Er1B–O7B 73.3(2) O2B–Er1B–O1B 74.05(9) O2B–Er1B–O4B 74.57(8) O2B–Er1B–O5B 139.59(9) O2B–Er1B–O7B 144.0(2)

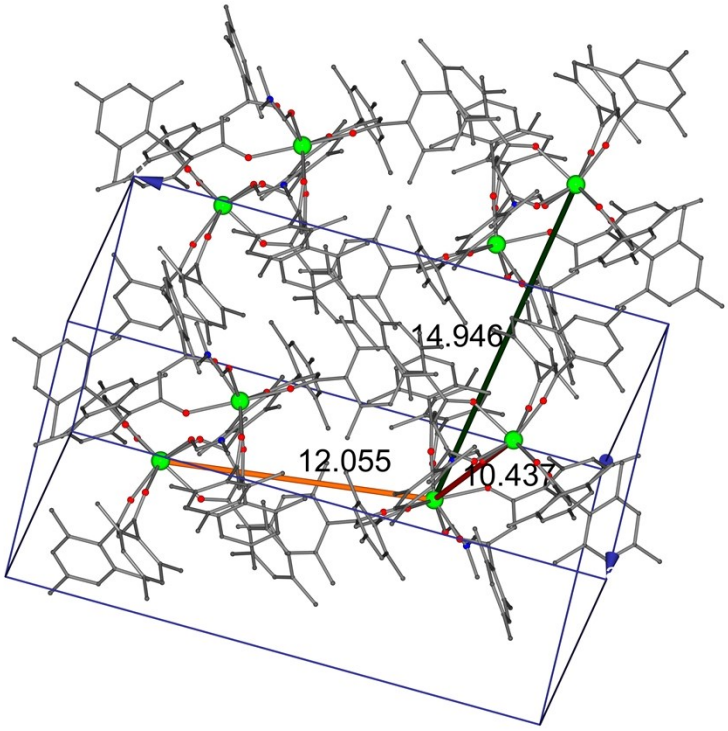

Fig. S14. Solid state packing diagram of complex **3** (viewed along the crystallographic *c* axis).

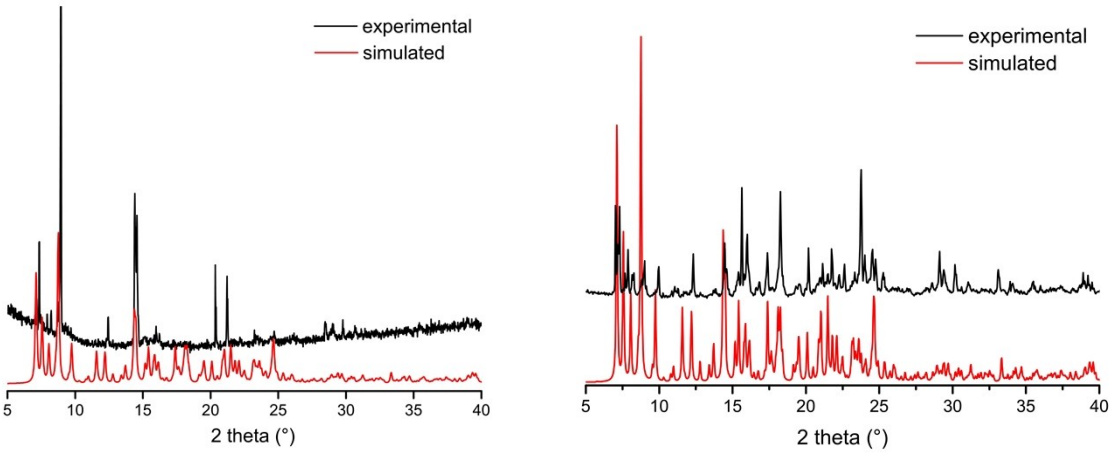

Fig. S15. The calculated and experimental PXRD pattern of complex **1** (*left*) and **3** (*right*).

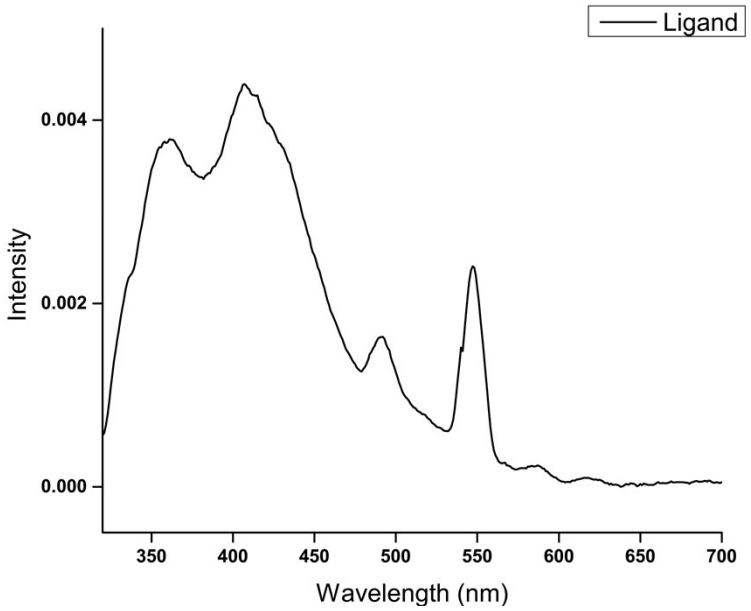

Fig. S16. Emission spectrum of ^{Mes}Acac.

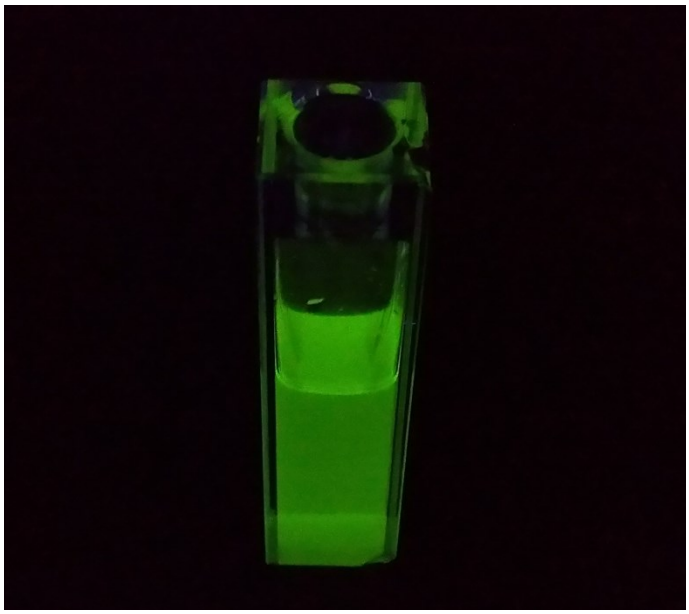

Fig. S17. Photographic image of complex **2** at 5 x 10^{-4} M concentration in DMF solution.

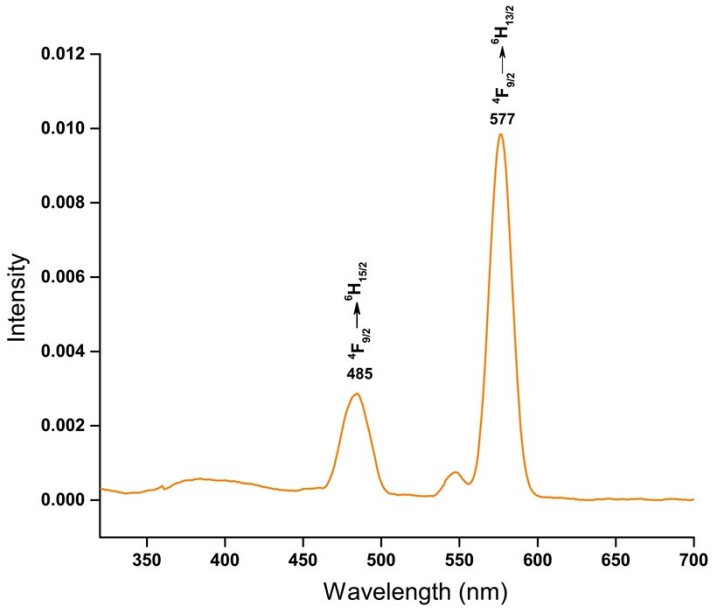

Fig. S18. Emission spectrum of the $Dy^{(III)}$ complex **1** (excitation at 305 nm; DMF solution 5 μM) at room temperature.

Table S3. Table of absolute quantum yield for **2**.

Sl. No.	Complex	Quantum Yield (%)
1	**2** (Tb)	0.74

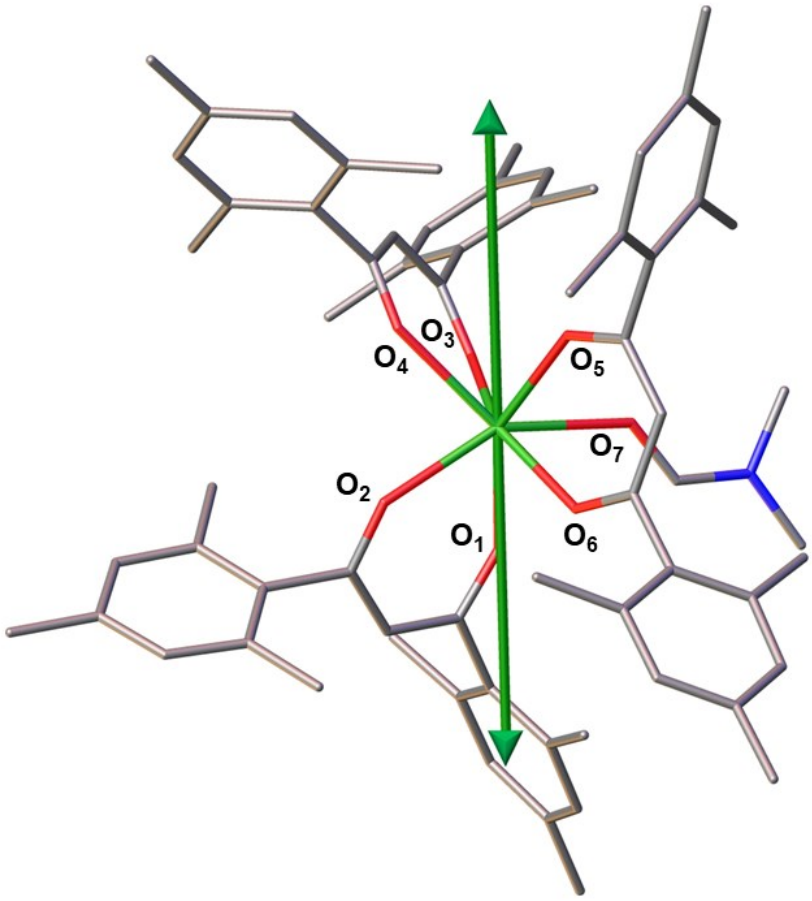

Fig. S19. Quantitative calculation of the anisotropic axes orientation (green arrows) using the electrostatic method by Chilton et al. (see ref. 26 in the manuscript).

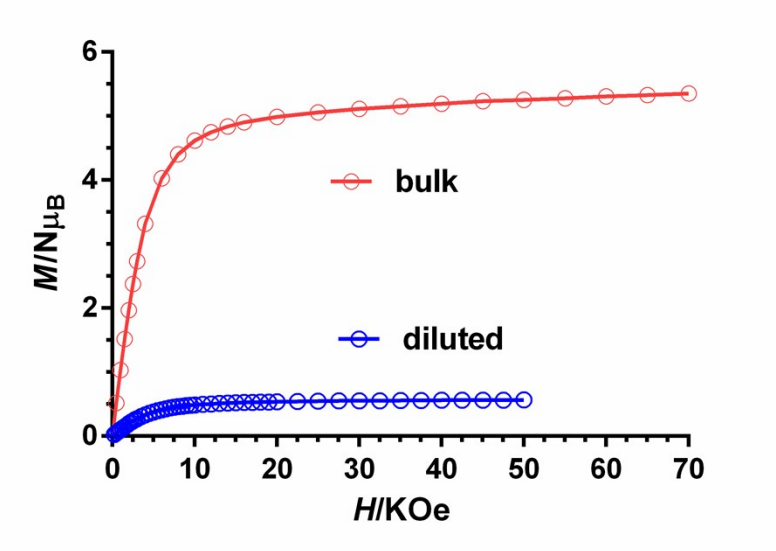

Figure S20. Field dependence of *M* for **1** and the diluted complex **3**.

Table S4. ANO-RCC basis set used in CASSCF calculation.

Atoms	Basis Set
H	2s
C	2s1p
N,O	3s2p1d
Dy, Tb, Er	8s7p5d3f2g1h

Table S5. The CASSCF computed energy (cm^{-1}) of the spin-free states for complex **1**. The red values represent the 21 sextets and grey values represent 224 quartets respectively for Dy^{III} ion.

Complex **1**					
0.000	25342.355	31157.687	38148.891	58069.030	79418.264
15.55856	25351.802	31160.378	38168.497	62467.481	85851.169
45.28642	25380.092	31167.919	38176.391	62467.611	85862.922
78.86821	25396.904	31169.427	43421.787	62589.279	86084.497
186.55344	25432.250	31179.558	43630.428	62595.696	86160.404
264.61617	25450.717	31183.030	43738.776	62639.740	86215.378
332.84645	25470.445	31246.756	43754.146	62658.545	88657.121
441.18351	25487.650	31254.800	43853.919	62672.563	88658.469
467.79481	25507.216	31268.787	43897.968	62688.306	88775.715
590.46138	25522.610	31274.825	43939.519	62725.362	88797.629
591.91869	25542.218	31289.047	45160.469	62769.116	88866.704
7515.51808	25564.242	31312.230	45162.778	62780.316	88921.386
7659.77437	25575.154	31320.893	45233.613	62869.598	88935.376
7716.13326	25585.362	31331.638	45238.249	62874.807	88990.607
7732.62678	25667.226	31336.671	45279.337	62920.470	89013.614
7802.31217	25677.177	31344.543	45282.596	62922.226	89129.214
7833.96041	25696.934	31345.869	45328.348	67690.754	89151.905
7850.16642	25712.607	33016.404	45341.351	67982.918	89193.814
34829.88655	26395.397	33056.621	45389.438	68085.580	89206.218
34947.64347	26425.735	33108.970	45472.099	73475.570	99292.812
35264.04468	26440.723	33210.708	45494.529	73560.069	99316.984
24839.27404	26446.221	33232.624	45523.586	73654.617	99553.916
24858.97189	26463.654	34529.133	45535.872	73880.204	99618.202
24878.02668	26492.754	34549.720	57536.238	73902.854	99726.114
24886.30965	26524.685	34556.054	57541.648	77448.934	99743.573
24907.2168	26572.950	34601.343	57614.537	77593.666	99848.587
24932.23691	26587.143	34621.556	57642.479	77593.985	106643.283
24976.5642	29712.214	34632.076	57662.126	77617.572	106652.533
24991.91426	29721.368	34655.810	57684.850	77635.099	106747.752
25015.8326	29725.712	34687.544	57703.723	77644.791	106758.151
25039.03985	29745.837	34699.755	57723.934	77660.246	106783.391
25064.4199	29765.654	34707.713	57744.807	77661.543	106846.123
25120.96534	29779.549	34724.244	57756.131	77674.260	106920.876
25137.76173	29793.060	37618.281	57789.094	77685.547	106948.179
25207.21668	29805.728	37732.317	57798.808	77699.730	106986.056
25230.13641	29827.491	37775.069	57849.441	77704.780	
25249.54675	29834.453	37825.767	57870.289	79066.482	
25271.43495	29847.428	37910.443	57881.732	79151.987	
25281.96096	29877.305	37974.181	57901.285	79184.945	
25297.38344	29900.451	38003.48094	57920.985	79218.580	
25307.48366	29933.530	38068.14036	57945.830	79261.768	
25330.38364	29937.935	38114.21687	58066.859	79380.923	

Table S6. The CASSCF computed energy (cm^{-1}) of the spin-free states for complexes **2** and **4.** The red values represent the 7 septets (for Tb^{III}) and 35 quartets (for Er^{III}) respectively. The grey values represent the 140 quintet and 112 doublet states for Tb^{III} and Er^{III} respectively.

Complex **2**				Complex **4**			
0.000	35329.616	50108.364	77478.760	0.000	18188.440	43986.668	60811.836
81.517	35384.698	50118.691	77500.122	18.183	18192.869	44047.916	60821.991
143.623	35556.796	50138.342	77579.787	69.743	18209.839	44077.387	60852.404
358.825	35580.498	50168.851	77627.994	93.065	18212.927	44161.266	60875.775
390.676	35634.374	50211.922	77692.160	97.916	23961.534	44166.154	60898.112
584.504	35647.785	50246.885	77733.978	277.157	23981.478	44181.690	77160.300
874.672	35670.547	50262.087	77862.836	300.586	23993.185	44185.005	77166.581
25690.613	40253.355	50313.810	93110.063	311.816	24037.657	44592.246	77240.584
25716.971	40269.028	50317.048	93119.621	338.834	24081.378	44593.011	77272.169
25748.170	40292.000	51722.003	93371.955	414.557	24094.174	44746.734	77331.562
25836.217	40307.567	51761.360	93398.774	459.388	24103.327	44750.563	77345.340
25842.069	40346.142	51910.970	93534.694	493.567	24166.237	44851.532	77362.382
29189.036	40356.938	51996.806	93566.140	534.485	24170.099	44855.089	77388.482
29194.230	40382.143	52168.262	93644.391	18293.965	26977.041	44927.922	77403.118
29198.768	40393.170	54523.700	93735.312	18307.123	26977.358	44947.412	110373.741
29203.838	40428.723	54711.112	93747.410	18346.357	27115.168	45010.796	110392.142
29265.830	40454.884	54781.364	95163.574	18415.536	27124.451	45030.966	110634.187
29283.090	40494.759	57634.318	95172.801	18423.769	27144.539	45072.849	110768.095
29333.920	40501.546	57661.153	95446.178	18428.041	27155.224	45123.953	110853.804
29349.057	40519.644	57668.929	95498.545	18507.582	27208.756	45139.855	110884.692
29364.506	40557.680	57750.986	95571.140	18718.774	27222.741	45181.131	111009.068
29406.966	40590.443	57771.691		28514.003	27273.121	45188.478	
29426.515	40601.554	57813.870		28569.331	27289.721	45207.555	
29578.459	40635.353	57849.990		28617.101	27311.601	45209.895	
29584.656	40679.999	57879.563		28842.643	27441.677	50180.459	
29630.974	40739.012	57884.649		28875.573	27448.949	50186.423	
29635.026	40745.360	57910.260		28941.952	27470.755	50228.883	
29645.539	45743.154	57960.548		28964.647	27474.812	50232.931	
29651.017	45755.793	68507.628		29001.292	33111.877	50253.040	
30598.926	45771.318	75031.557		29046.637	33136.483	50270.566	
30641.821	45811.833	75055.721		46627.195	33166.269	50273.442	
30659.667	45846.109	75074.925		46900.377	33254.722	50285.706	
30745.918	45866.801	75091.449		46973.790	33274.043	50347.029	
30771.387	45872.280	75099.409		47149.019	33328.465	50366.915	
30799.480	45905.706	75126.441		47282.433	33379.964	50391.463	
30808.277	45925.788	75197.211		18108.725	33382.183	51414.549	
30857.683	45928.350	75210.217		18115.393	43823.198	51464.465	
30876.467	45945.619	75254.220		18120.801	43830.528	51613.523	
35228.715	45963.911	75291.402		18131.178	43880.553	51635.241	
35259.037	45978.199	75325.864		18147.996	43889.801	51711.694	
35288.993	46047.892	75349.211		18175.216	43945.577	60712.677	
35304.867	46048.789	75356.555		18178.902	43962.419	60788.392	

Table S7. The CASSCF computed energy (cm^{-1}) of the low lying spin-orbit states for complexes **1**, **2**, and **4**.

Complex **1**	Complex **2**	Complex **4**
0.000	0.000	0.000
0.000	2.386	0.000
44.462	42.233	44.122
44.462	48.228	44.122
144.579	157.180	72.850
144.579	176.558	72.850
183.828	234.502	85.383
183.828	272.181	85.383
246.009	292.166	233.499
246.009	311.292	233.499
282.214	322.264	251.698
282.214	458.891	251.698
363.743	461.487	352.192
363.743		352.192
527.444		389.348
527.444		389.348

Table S8. SINGLE_ANISO computed *g*-values, tunneling gap Δ_{tun} (for non KDs of Tb^{III} in complex **2**) and the angle of deviation from ground state g_{zz} orientation of low-lying eight Kramers doublet for Er^{III} ion in complex **4** respectively.

Complex 2		
$\pm M_J$ *states* (from 7 Septets+ 140 Quintets)	g_{xx}; g_{yy}; g_{zz}	Δ_{tun}
0.000	0.000; 0.000;15.483	2.386
42.233	0.000; 0.000; 12.736	5.995
157.180	0.000; 0.000; 10.862	19.378
272.181	0.000; 0.000; 13.324	19.985
311.292	0.000; 0.000; 12.606	10.972
458.891	0.000; 0.000;17.217	2.596
Complex 4		
$\pm M_J$ *states* (from 35 Quartets + 112 Doublets)	g_{xx}; g_{yy}; g_{zz}	θ (^{o} *angle*)
0.0	0.311; 0.563; 15.156	0
44.122	9.045; 7.062; 0.395	106.0
72.850	0.391; 0.935; 5.882	113.0
85.382	0.444; 7.237; 12.678	118.1
233.499	9.416; 6.053; 1.016	38.0
251.698	9.599; 6.085; 1.173	39.1
352.192	0.837; 1.421; 14.383	67.3
389.348	0.465; 1.695; 15.520	31.8

Table S9. SINGLE_ANISO computed wave function decomposition analysis for Dy(III) in complex **1**. The major dominating values are kept in bold.

$\pm M_J$	*wave function decomposition analysis*
KD1	**78.9% |±15/2⟩** + 10.6% |±11/2⟩ + 6.6 % |±7/2⟩ + 2.9 % |±5/2⟩
KD2	**53.4% |±3/2⟩** + 46.2% |±1/2⟩ + 40.2% |±5/2⟩ + 31.4% |±7/2⟩ + 17.2% |±9/2⟩ + 8.2% |±11/2⟩
KD3	**67.6% |±13/2⟩** + 27.1% |±3/2⟩ + 24.0% |±9/2⟩ + 21.1% |±5/2⟩ + 17.0% |±7/2⟩
KD4	**36.6% |±7/2⟩** + 36.4% |±13/2⟩ + 28.2% |±9/2⟩ + 25.4% |±3/2⟩ + 25.3% |±1/2⟩ + 18.0% |±5/2⟩
KD5	**55.0% |±11/2⟩** + 38.7% |±3/2⟩ + 33.0% |±1/2⟩ + 28.5% |±5/2⟩ + 17.6% |±7/2⟩ + 11.8% |±9/2⟩ + 4.3% |±3/2⟩
KD6	**55.6% |±9/2⟩** + 36.0% |±11/2⟩ + 31.6% |±13/2⟩ + 30.1% |±5/2⟩ + 18.8% |±3/2⟩ + 5.5% |±1/2⟩
KD7	**22.8% |±1/2⟩** + 26.6% |±5/2⟩ + 25.5% |±3/2⟩ + 3.1% |±7/2⟩
KD8	**49.0%|±5/2⟩** + 47.9% |±3/2⟩ + 39.4% |±1/2⟩ + 8.0% |±13/2⟩ + 7.3% |±7/2⟩ + 4.6% |±9/2⟩ + 2.4% |±11/2⟩

Table S10. SINGLE_ANISO computed wavefunction decomposition analysis for Tb(III) in complex **2**. The major dominating values are kept in bold.

$\pm M_J$	*wave function decomposition analysis*
1	**55.3% |±6⟩** + 33.9% |±4⟩ + 20.8 % |±5⟩ + 14.3% |±2⟩ + 14.3% |±2⟩ + 2.7% |±3⟩
2	**55.2% |±5⟩** + 36.0% |±3⟩ + 15.0% |±4⟩ + 12.3% |±1⟩
3	**43.6% |±4⟩** + 35.3% |±2⟩ + 14.6% |±1⟩ + 5.4% |±3⟩
4	**49.9% |±1⟩** + 34.6% |±3⟩ + 24.4% |±5⟩ + 21.3% |±4⟩ + 8.9% |±0⟩
5	**49.6% |±3⟩** + 33.5% |±1⟩ + 29.3% |±5⟩ + 11.1% |±4⟩ + 16.2% |±2⟩+1.8% |0⟩
6	**44.1% |±2⟩** + 31.5% |±1⟩ + 27.1% |±4⟩ + 14.7% |±3⟩ + 6.5% |±6⟩+0.8% |±5⟩

Table S11. SINGLE_ANISO computed wave function decomposition analysis for Er(III) in complex **4**. The major dominating values are kept in bold.

$\pm M_J$	*wave function decomposition analysis*

KD1	**54.8% |±15/2⟩** + 35.6 % |±11/2⟩ + 20.2% |±9/2⟩ + 15.6% |±5/2⟩ + 9.9% |±13/2⟩ + 5.5% |±7/2⟩
KD2	**40.6% |±9/2⟩** + 34.2% |±13/2⟩ + 32.9% |±5/2⟩ + 17.8% |±3/2⟩ + 16.5% |±11/2⟩ + 6.7% |±7/2⟩
KD3	**39.9% |±7/2⟩** + 38.8% |±13/2⟩ + 29.3% |±1/2⟩ + 21.1% |±11/2⟩ + 12.9% |±9/2⟩ + 12.9% |±9/2⟩
KD4	**44.6% |±5/2⟩** + 37.7% |±3/2⟩ + 28.1% |±11/2⟩ + 27.0% |±13/2⟩ + 26.0% |±1/2⟩+14.0% |±9/2⟩
KD5	**48.2% |±1/2⟩** + 37.8% |±3/2⟩ + 36.2% |±9/2⟩ + 23.1% |±11/2⟩ + 9.6% |±5/2⟩
KD6	**30.2% |±11/2⟩** + 29.0% |±1/2⟩ + 28.5% |±5/2⟩ +5.9 % |±3/2⟩
KD7	**34.1% |±3/2⟩** + 32.0% |±5/2⟩ + 25.9% |±11/2⟩ + 16.3% |±7/2⟩ + 6.2% |±13/2⟩
KD8	**52.5% |±13/2⟩** + 45.4% |±11/2⟩ + 29.7% |±9/2⟩ + 19.6% |±5/2⟩ + 9.5% |±3/2⟩

Table S12. SINGLE_ANISO computed crystal field parameters for **1**, **2**, and **4**. The major components in the Table are in bold.

		Complex 1	**Complex 2**	**Complex 4**
k	**q**	B_k^q	B_k^q	B_k^q
2	-2	-0.19E+01	**0.39E+01**	0.26E+00
	-1	**0.80E+01**	0.59E+00	-0.60E+00
	0	**-0.24E+01**	**-0.24E+01**	-0.32E+00
	2	**-0.41E+01**	-0.43E+00	**0.19E+01**
	1	**-0.48E+01**	0.19E+00	-0.25E+00
4	-4	0.49E-01	0.41E-01	-0.26E-02
	-3	0.20E+01	-0.15E+00	-0.45E-01
	-2	0.10E+01	-0.42E-01	-0.81E-02
	-1	-0.14E+01	-0.15E-01	-0.23E-01
	0	-0.45E+01	0.19E-02	-0.90E-03
	1	0.32E+00	0.45E-01	0.17E-01
	2	0.52E+00	0.45E-01	0.18E-01
	3	0.27E+00	0.55E-01	-0.49E-01
	4	0.13E+00	-0.12E-01	-0.13E-01
	-6	-0.81E-03	0.11E-03	0.12E-03
	-5	-0.17E-01	0.68E-03	-0.13E-02

6	-4	0.22E-02	-0.63E-04	-0.21E-03
	-3	-0.25E-02	0.35E-03	-0.53E-03
	-2	0.52E-03	0.51E-04	-0.49E-03
	-1	0.39E-02	-0.48E-04	0.31E-03
	0	0.41E-03	0.21E-04	-0.19E-04
	1	-0.52E-02	-0.11E-04	0.31E-03
	2	-0.35E-02	-0.23E-03	-0.34E-04
	3	0.12E-02	-0.12E-03	0.19E-03
	4	-0.34E-02	0.63E-04	0.53E-04
	5	-0.18E-02	-0.12E-03	0.32E-03
	6	0.56E-02	0.44E-03	0.73E-04

Table S13. CASSCF computed LoProp charges on coordinated ligand atoms.

Atoms	**1**	**2**	**4**
O1	-0.7521	-0.7432	-0.7166
O2	-0.7052	-0.7011	-0.7201
O3	-0.7456	-0.7441	-0.7305
O4	-0.6961	-0.7220	-0.7565
O5	-0.7240	-0.7211	-0.7253
O6	-0.7164	-0.7095	-0.6934
O7	-0.6545	-0.6564	-0.6611

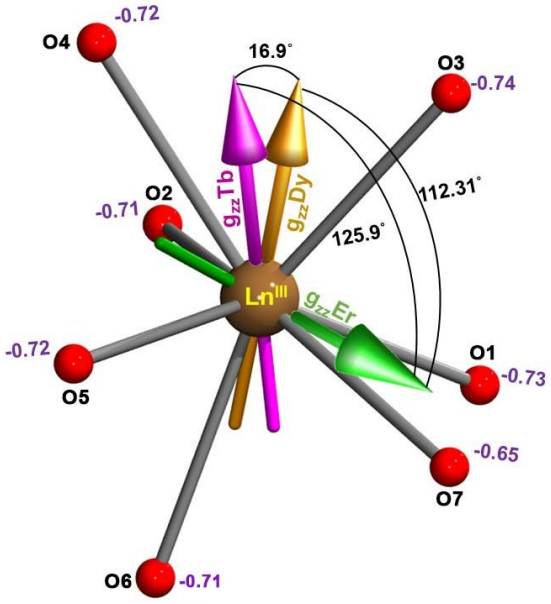

Fig. S21. Orientation of ground state g_{zz} axes on the Ln(III) ion in complexes **1**, **2**, and **4**. The purple values represent the average LoProp charges on the oxygen donor atoms.

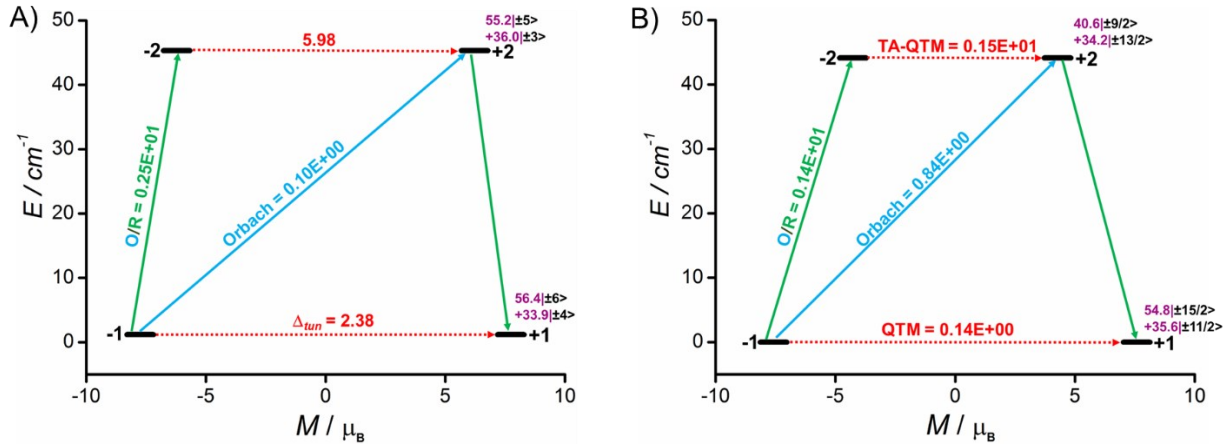

Fig.S22. The plausible magnetic relaxation mechanism in complexes **2** (A) and **4** (B). The red dotted arrows show the magnetic relaxation via QTM (between ground KDs) and TA-QTM (between excited state KDs) respectively in complex **4** while Δ_{tun} represent the tunneling splitting between the non KDs in complex **2**. The green and sky blue arrows represent the magnetic relaxation through Orbach and Orbach/Raman processes. The purple characters represent the composition of M_J states.